JOURNAL OF SOLID STATE CHEMISTRY 117, 213–216 (1995)

BRIEF COMMUNICATION

Synthesis and Structure of the Layered Quadruple Perovskite $Tb_2Ba_2Cu_2Ti_2O_{11}$

M. R. Palacín, F. Krumeich,* M. T. Caldés, and P. Gómez-Romero[1]

*Institut de Ciència de Materials de Barcelona (CSIC), Campus Universitario, Universidad Autónoma de Barcelona, E-08193 Bellaterra, Barcelona, Spain; and *Institut für Anorganische Chemie, AG Festkörperanalytik, Römerstrasse 164 D-53117 Bonn, Germany*

Received June 21, 1994; in revised form October 14, 1994; accepted October 18, 1994

The synthesis, structure, and high-resolution transmission electron microscopy studies of the layered quadruple perovskite $Tb_2Ba_2Cu_2Ti_2O_{11}$ are reported. This oxide represents the limit of the series $Ln_2Ba_2Cu_2Ti_2O_{11}$, Tb being the smallest lanthanide compatible with the stability of the $a_p \times a_p \times 4a_p$ superstructure observed (a_p = cubic perovskite cell length). This structure was confirmed by powder X-ray diffraction profile analyses, electron diffraction, and high-resolution electron microscopy. The Cu-O (basal) bond distance of 1.947(3) Å and the Cu–O–Cu bond angle of 169(1)° are the best suited within this series of oxides to the attainment of superconductivity upon appropriate *p*-doping. © 1995 Academic Press, Inc.

INTRODUCTION

Despite the early discovery of the ordered defect perovskite structure of $YBa_2Cu_3O_{7-\delta}$, the search for new high-T_c superconductors has centered much more frequently on perovskite/NaCl-like intergrowths than on all-perovskite oxides. The control of dimensionality and order in the perovskite structure represents a difficult challenge, and work in this direction has centered mostly on the synthesis of 123 derivatives where the CuI ions, forming CuO chains, would be replaced by other metals such as Nb and Ta (1–6), Al (7), Ga (8, 9), Fe (10), and Co (11–15). More recently, other novel types of perovskite superstructures leading to bidimensionality have been reported (16, 17). Furthermore, a recent report on the possibility of high-T_c superconductivity in three-dimensional perovskites in the system Ba–Pb–Tl–Cu–O has reopened the debate on the importance of bidimensionality for high-T_c superconductivity (18).

In our particular search for superconductivity, we have centered on the development of new all-perovskite phases in the systems *Ln*–A–Cu–M–O (where *Ln* denotes a lanthanide, *A* denotes an alkaline earth, and *M* denotes an early transition metal). Thus, we have studied the disordered three-dimensional perovskite La_2CuTiO_6 (19–21) and have recently reported the induction of order and bidimensionality in this system, as found in the series $Ln_2Ba_2Cu_2Ti_2O_{11}$ (*Ln* = La,Nd,Eu) (22). Another work reporting the related $Gd_2Ba_2Cu_2Ti_2O_{11}$ has also appeared (23). We report here the synthesis and structure of the terbium derivative, the last member of this series, corresponding to the lanthanide with the smallest size compatible with the existence of the structure and presenting the shortest Cu–O(basal) distance within the series.

EXPERIMENTAL

$Tb_2Ba_2Cu_2Ti_2O_{11}$ was prepared by solid-state reaction of stoichiometric amounts of TiO_2, CuO, $BaCO_3$, and $Tb_2(CO_3)_3$, all purchased from Aldrich or Baker and all of purity ≥99.9%. To ensure its purity, $BaCO_3$ was treated at 200°C for 2 days. The synthesis was carried out in two steps of 24 hr each with an intermediate regrinding. The first step consisted of 2 hr at 900°C to allow the carbonates to decompose plus 24 hr at 1100°C. The second step consisted of a single heating run at 1100°C for 24 hr. The heating and cooling rates were both 100°C/hr. The determination of the oxygen content of the samples was made by thermogravimetric analyses in Ar(95%)/H_2(5%) atmosphere at 650°C using a PE TGA7 balance (maximum sensitivity 0.1 μg) and normally using ca. 40 mg of sample.

X-ray powder diffraction patterns were obtained using Cu$K\alpha$ radiation with a Siemens D-500 diffractometer (λ = 1.5418 Å). Data were collected from 2θ 2.0° to 60.00° with a step of 0.02° and with 8 sec counting time per step. Rietveld profile analyses were performed with the help of the program FULLPROF (24). Electron microscopic in-

[1] To whom correspondence should be addressed.

0022-4596/95 $6.00

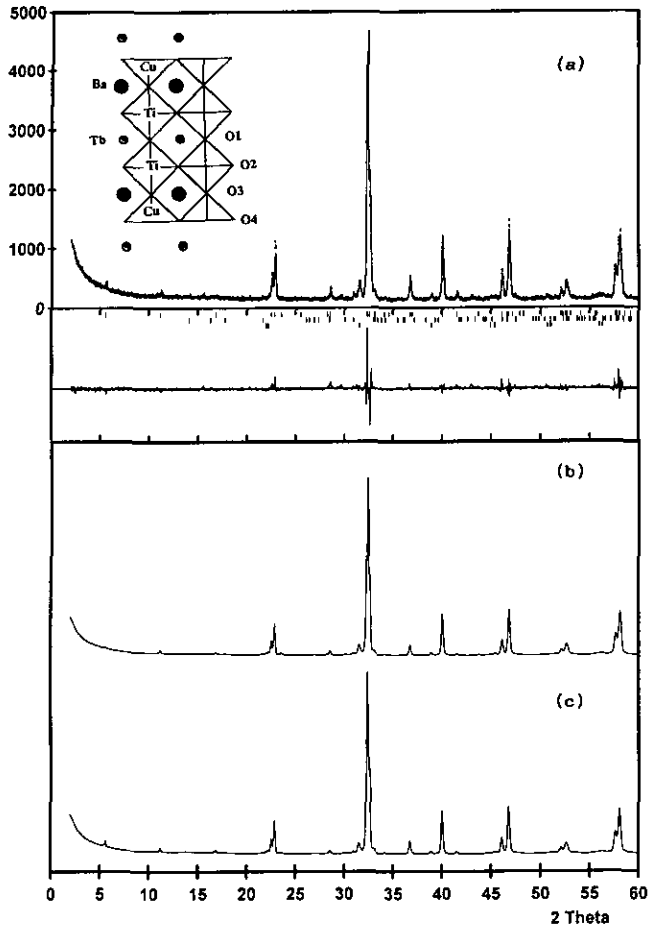

FIG. 1. (a) Results of the X-ray profile analysis for $Tb_2Ba_2Cu_2Ti_2O_{11}$. The experimental diffractogram (dots), the calculated profile (continuous line), and the difference between them (bottom line) are represented. Small vertical bars mark the positions of allowed Bragg reflections for the title oxide (top) and for small amounts of $Tb_2Cu_2O_5$ (middle) and $BaTiO_3$ (bottom) impurities. (b) Calculated profile for an ideally disordered model. (c) Calculated profile for an ordered model. Patterns (b) and (c) were calculated using realistic background, profile parameters, and impurity contributions as obtained from the experimental diffractogram.

vestigations were carried out on a CM30ST transmission electron microscope (Philips) working at 300 kV. The simulated HRTEM images were calculated with the program package EMS (25).

RESULTS AND DISCUSSION

The title oxide represents the limit of the series $Ln_2Ba_2Cu_2Ti_2O_{11}$ since terbium is the smallest lanthanide (*Ln*) compatible with the isolation of this phase. Dysprosium and smaller ions led to mixtures of binary oxides (26). From thermogravimetric analysis, the oxygen content of this oxide was found to be 10.95 ± 0.02 per formula unit.

The X-ray diffraction pattern (Fig. 1a) can be indexed with a tetragonal unit cell (a = 3.8769(1) Å, c = 15.7322(7) Å) corresponding to a quadruple perovskite lattice similar to those found for the related La, Nd, and Eu derivatives, but with a larger tetragonal distortion in the present case.

The weak 001 peak at $2\theta = 5.62°$ is the first indication of a superstructure with oxygen vacancies arranged in planes and cation order as confirmed from neutron diffraction data for the neodymium derivative (27). Nevertheless, Cu/Ti and Tb/Ba are pairs close enough in atomic number to make difficult a quantitative analysis of their distribution on the structure from X-ray data alone. This is illustrated by the two calculated diffractograms shown in Figs. 1b and 1c, corresponding to disordered and ordered arrangements of the metal ions in the tetragonal structure, respectively. It is evident that the differences are minimal and involve mainly the low-angle superstructure peaks. We believe that in the absence of these, the result of a Rietveld profile refinement, such as that reported in Ref. (23), would be quite insensitive to the order of the structural model used.

It is with this in mind that the results of the profile analysis shown in Fig. 1a have to be considered. The

TABLE 1
Final Refined Atomic Parameters for $Tb_2Ba_2Cu_2Ti_2O_{11}$[a]

Name	Site	x (σx)	y (σy)	z (σz)	B(Å^2) (σB)	Occupancy[b]
Tb1	1c	0.50000(0)	0.50000(0)	0.00000(0)	0.5(4)	1.000
Ba2	2h	0.50000(0)	0.50000(0)	0.2343(4)	1.2(2)	2.000
Tb3	1d	0.50000(0)	0.50000(0)	0.50000(0)	2.0(4)	1.000
Ti	2g	0.00000(0)	0.00000(0)	0.372(14)	1.7(3)	2.000
Cu	2g	0.00000(0)	0.00000(0)	0.110(1)	1.7(3)	2.000
O1	1b	0.00000(0)	0.00000(0)	0.50000(0)	1.1(4)	1.000
O2	4i	0.00000(0)	0.50000(0)	0.395(2)	1.1(4)	4.000
O3	2g	0.00000(0)	0.00000(0)	0.266(1)	1.1(4)	2.000
O4	4i	0.00000(0)	0.50000(0)	0.098(2)	1.1(4)	4.000

[a] Space group *P4/mmm*. Cell parameters: a = 3.8769(1) Å, c = 15.7322(7) Å.
[b] Atoms per unit cell. All values were fixed.

TABLE 2
Selected Bond Distances (Å) and Angles (°) for $Tb_2Ba_2Cu_2Ti_2O_{11}$

Tb1–O4	8×	2.48(2)	Ti–O1	1×	2.01(2)
Ba2–O2	4×	3.18(3)	Ti–O2	4×	1.971(7)
Ba2–O3	4×	2.786(3)	Ti–O3	1×	1.67(3)
Ba2–O4	4×	2.89(2)			
Tb3–O1	4×	2.7414(1)	Cu–O3	1×	2.45
Tb3–O2	8×	2.55(2)	Cu–O4	4×	1.947(3)
O1–Ti–O2		80(1)	O3–Cu–O4		95(1)
O1–Ti–O3		180	O4–Cu–O4		169(1)
O2–Ti–O2		159(2)	O4–Cu–O4		89.5(1)
O2–Ti–O2		88.1(3)			
O2–Ti–O3		100(2)	Ti–O2–Ti		159(2)
			Cu–O4–Cu		169(1)

ordered structural model refined was similar to that obtained for the analogous Eu derivative and was satisfactory in general, except for the position of O3, which refined systematically away from Cu and too close to Ti and was consequently forced into a position 2.45 Å away from the former. Furthermore, other attempts to refine disorder parameters failed, indicating the relatively low sensitivity of powder X-ray diffraction to these fine structural details. Thus, in contrast to the results reported in Ref. (23) for the Gd derivative, our refinement with a disordered O2 showed no stable shift of its position and finally led (when the shift was considerably dampened) to a slightly worse model, according to the reliability factors. Equally unsatisfactory were attempts to refine a disordered distribution of Tb and Ba, which resulted in negative occupancy factors for some of these atoms. The final refined model therefore included occupancy factors corresponding to the ordered layered distribution, which is also deduced from high-resolution electron microscopy (see below). The final reliability factors were $R_p = 8.51$, $R_{wp} = 11.2$, $R_{expected} = 6.38$, and $\chi^2 = 3.07$; their definitions are the same as those given in Ref. (22). Table 1 shows the final atomic parameters obtained, and Table 2 lists selected bond distances and angles. Among the most significant we can see the Cu–O4 distance of 1.947(3) Å corresponding to the shortest Cu–O (equatorial) bond length within the series. Aside from magnetic considerations, from a structural point of view, this short distance together with the large Cu–O–Cu angle (169(1)°) makes this derivative the best candidate within the family of quadruple perovskite oxides for presenting high-temperature superconductivity upon suitable *p* doping (28).

The layered structure of the title oxide can be also confirmed and analyzed by electron diffraction and high-resolution electron microscopy (see Fig. 2). First, the electron diffraction pattern shown (zone axis [100]) clearly presents the $a_p \times a_p \times 4a_p$ superstructure. This is further detailed with the high-resolution images. Furthermore, simulation of the high-resolution image, as obtained from the refined positional parameters in Table 1 (see also inset Fig. 2), confirms definitively the layered arrangement of oxygen vacancies and the ordered distribution of cations in the title oxide.

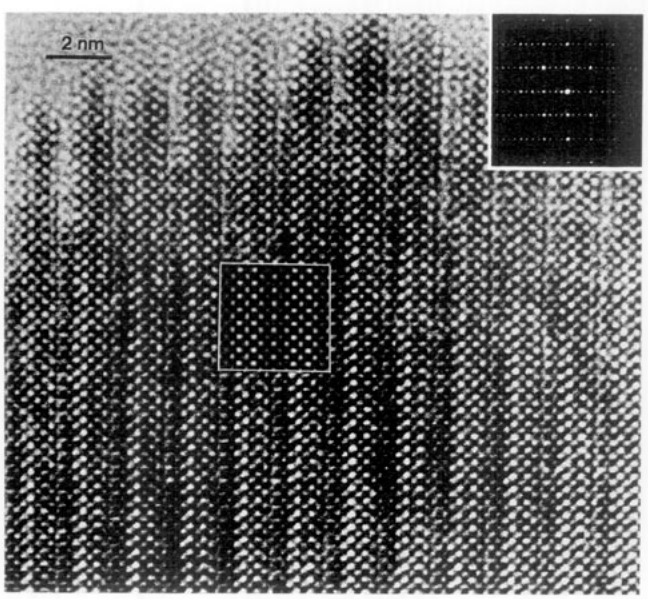

FIG. 2. High-resolution transmission electron microscope image for $Tb_2Ba_2Cu_2Ti_2O_{11}$ (along [100]) with inserted simulation (defocus, 30 nm; thickness, 3.9 nm) and electron diffraction pattern. The image simulation contains two unit cells along *c* (vertical) and eight along *b* (horizontal), with the oxygen vacancy at the origin. In addition to the evident layered structure, the image simulation calculated from the ordered structural model obtained, as given in Table 1, confirms the ordered model proposed.

ACKNOWLEDGMENTS

We thank the Spanish DGICYT (PB93-0122), CICYT (MAT93-0240-C04-01) and the MIDAS Program (92-1592) for financial support, and the Generalitat de Catalunya for a predoctoral fellowship awarded to M.R.P. We also thank the German and Spanish governments (SGCCT, MAE) for a joint project (CSIC-Kernforschungszentrum Karlsruhe).

REFERENCES

1. N. Murayama, E. Sudo, K. Kani, A. Tsuzuki, S. Kawakami, M. Awano, and Y. Torii, *Jpn. J. Appl. Phys.* **27**(9), L1623 (1988).
2. C. Greaves and P. R. Slater, *Physica C* **161,** 245 (1989).
3. M. J. Rey, P. Dehaudt, J. Joubert, and A. W. Hewat, *Physica C* **167,** 162 (1990).
4. C. Greaves and P. R. Slater. *IEEE Trans. Magn.* **27**(2), 1174 (1991).
5. H. W. Zandbergen, R. J. Cava, J. J. Krajewski, and W. F. Peck, Jr., *J. Solid State Chem.* **101,** 322 (1992).
6. B. Hellebrand, X. Z. Wang, and P. L. Steger, *J. Solid State Chem.* **110,** 32 (1994).

7. S. A. Sunshine, L. F. Schneemeyer, T. Siegrist, D. C. Douglass, J. V. Waszczak, R. J. Cava, E. M. Gyorgy, and D. W. Murphy, *Chem. Mater.* **1,** 331 (1989).
8. J. T. Vaughey, J. P. Thiel, E. F. Hasty, D. A. Groenke, C. L. Stern, K. R. Poeppelmeier, B. Dabrowski, D. G. Hinks, and A. W. Mitchell, *Chem. Mater.* **3,** 935 (1991).
9. G. Roth, P. Adelmann, G. Heger, R. Knitter, and Th. Wolf, *J. Phys. I Fr.* **1,** 721 (1991).
10. P. R. Slater and C. Greaves, *Physica C* **180,** 299 (1991).
11. P. F. Miceli, J. M. Tarascon, L. H. Greene, P. Barboux, F. J. Rotella, and J. D. Jorgensen, *Phys. Rev. B* **37,** 5932 (1988).
12. Y. K. Tao, J. S. Swinnea, A. Manthiram, J. S. Kim, J. B. Goodenough, and H. Steinfink, *J. Mater. Res.* **3,** 248 (1988).
13. M. S. Hedge, K. M. Satyalakshmi, S. Ramesh, N. Y. Vasanthacharya, and J. Gopalakrishnan, *Mater. Res. Bull.* **27,** 1099 (1992).
14. Q. Huang, R. J. Cava, A. Santoro, J. J. Krajewski, and W. F. Peck, *Physica C* **193,** 196 (1992).
15. T. A. Mary, N. R. S. Kumar, and U. V. Varadaraju, *J. Solid State Chem.* **107,** 524 (1993).
16. M. T. Anderson and K. R. Poeppelmeier, *Chem. Mater.* **3,** 476 (1991).
17. M. T. Anderson, K. R. Poeppelmeier, J.-P. Zhang, H.-J. Fan, and L. D. Marks, *Chem. Mater.* **4,** 1305 (1992).
18. V. Manivannan, J. Gopalakrishnan, and C. N. R. Rao, *J. Solid State Chem.* **109,** 205 (1994).
19. P. Gómez-Romero, M. R. Palacín, N. Casañ, A. Fuertes, B. Martínez, *Solid State Ionics* **63–65,** 424 (1993).
20. M. R. Palacín, J. Bassas, J. Rodríguez-Carvajal, and P. Gómez-Romero, *J. Mater. Chem.* **3**(11), 1171 (1993).
21. M. R. Palacín, J. Bassas, J. Rodríguez-Carvajal, A. Fuertes, N. Casañ-Pastor, and P. Gómez-Romero, *Mater. Res. Bull.* **29**(9), 973 (1994).
22. M. R. Palacín, A. Fuertes, N. Casañ-Pastor, and P. Gómez-Romero, *Adv. Mater.* **6**(1), 54 (1994).
23. A. Gormezano and M. T. Weller, *J. Mater. Chem.* **3**(7), 771 (1993).
24. J. Rodríguez-Carvajal, PROGRAM FULLPROF (Version 2.5, April 1994, ILL), unpublished 1994.
25. P. Stadelmann, *Ultramicroscopy* **21,** 131 (1987).
26. M. R. Palacín, A. Fuertes, N. Casañ-Pastor and P. Gómez-Romero, submitted for publication.
27. P. Gómez-Romero, M. R. Palacín, and J. Rodríguez-Carvajal, *Chem. Mater.* **6**(11), 2118 (1994).
28. During the process of publication of this article several preliminary attempts to dope the series $Ln_2Ba_2Cu_2Ti_2O_{11}$ have been carried out. We note that some of the simplest doping schemes such as substitution of A^{2+} for Ln^{3+} are not feasible. We are currently working on more elaborate doping schemes.